Earth and Planetary Science Letters 331–332 (2012) 120–127

Contents lists available at SciVerse ScienceDirect

Earth and Planetary Science Letters

journal homepage: www.elsevier.com/locate/epsl

Salt lake deformation detected from space

J. Ruch [a,*], J.K. Warren [b], F. Risacher [c], T.R. Walter [d], R. Lanari [e]

[a] Dipartimento di Scienze Geologiche, Roma Tre, Italy
[b] Dept. of Geology, Faculty of Science, Chulalongkorn University, Bangkok, Thailand
[c] IRD, CNRS, France
[d] Helmholtz Centre Potsdam, GFZ German Research Centre for Geosciences, Germany
[e] IREA, CNR, Italy

ARTICLE INFO

Article history:
Received 27 September 2011
Received in revised form 8 February 2012
Accepted 2 March 2012
Available online xxxx

Editor: P. DeMenocal

Keywords:
InSAR
central Andes
salar
salt flat
halite
ground deformation

ABSTRACT

To investigate the spatiotemporal evolution of salars in the Atacama Desert in Chile (24–26°S), we use a deformation time series retrieved by applying satellite radar interferometry techniques for the period from 2003 to 2008. We find that all 12 salars surveyed are actively deforming, with displacement rates from −1.4 to 1.5 cm/yr in the satellite line-of-sight direction. Displacement rates are mostly confined to the salars themselves, and are generally constant in time and space. To understand the reason for this displacement signal, we further compare these observations with LANDSAT imagery and field observations. Relationships between these observations suggest that the most rapid uplift regions indicate subsurface material accretion. A variety of saline sedimentary processes related to the salar hydrology can explain this accretion, the most likely being capillary halite precipitation within and below surficial salt crusts. We further propose that salars, whose dynamics are dependent on the presence of brine and resurging saline groundwater, may be used as potential indicators of water resource evolution in the central Andes, and in similar water-limited regions elsewhere on earth.

© 2012 Elsevier B.V. All rights reserved.

1. Introduction

Dry lakes and saline lakes are common geomorphologic features in arid regions and are known to be reliable indicators of hydrology using both field and remote sensing technologies. Morphologically, saline hydrologies accumulating bedded salts typically occur in hydrographically-closed depressions or saline pans, which are infrequently water covered, but act as continual groundwater sumps, even when the salar surface is subaerial (Warren, 2010). Sedimentologically, within a broad range of saline depressions worldwide, salars define a particular style of saline sump where halite precipitates near the upper surface of the groundwater system, via the evaporation of groundwater brines (Jordan et al., 2002; Lowenstein et al., 2003).

Elevation changes at salar surfaces have been observed using InSAR in the central Andes (Pritchard, 2003), however, no clear explanations have been yet provided to explain the deformation mechanisms. The present study utilises an InSAR time series across a number of salars to show that the ground surface within a salar is subject to variable displacement rates tied to specific sedimentary units and their inherent hydrological processes.

1.1. Climatic and sedimentologic framework

Altiplano Puna encompasses substantial portions of the hyperarid Atacama Desert; one of the driest regions of the world with an average elevation of 3750 m (Fig. 1a, Strecker et al., 2007). A hyperarid desert, by definition, experiences a number of consecutive years with no rain. Salts are accumulating in various forms and geometries across the Atacama Desert, for example: 1) as a suite of sodium-nitrate salts in pedogenic horizons; 2) as calcium-sulphate mantles on newly formed volcanic cones, and 3) as thick beds of salar halite in intermontane groundwater sumps (Warren, 2006). Hereafter we concentrate on this third group. During the Mid-Holocene period, the Altiplano Puna plateau underwent rapid regional climatic change, with many areas shifting from vegetated regimes, subject to more frequent rainfall, to inhospitable hyperarid desertic environments (Betancourt et al., 2000; Núñez et al., 2002; Placzek et al., 2006; Quade et al., 2008). In response to the desertification, the regional water table was lowered and many former perennial intermontane saline lakes desiccated into salars (Bobst et al., 2001; Lowenstein et al., 2003).

The term salar describes a groundwater sump where the sediments are typically subaerial and halite-rich, with intrasediment salt-growth textures driven by capillary evaporation of near-surface hypersaline groundwaters (Fig. 1b; Lowenstein and Hardie, 1985; Alonso et al., 1991; Warren, 2006, 2010). In a salar centre (depression), the hypersaline water table is less than a metre beneath the halite-encrusted salar

* Corresponding author at: Dipartimento di Scienze Geologiche, Universita' Roma Tre, 1, Lungo S.L. Murialdo, 00146 Rome, Italy. Tel.: +39 065 733 8012; fax: +39 065 733 80.
E-mail address: jruch@uniroma3.it (J. Ruch).

0012-821X/$ – see front matter © 2012 Elsevier B.V. All rights reserved.
doi:10.1016/j.epsl.2012.03.009

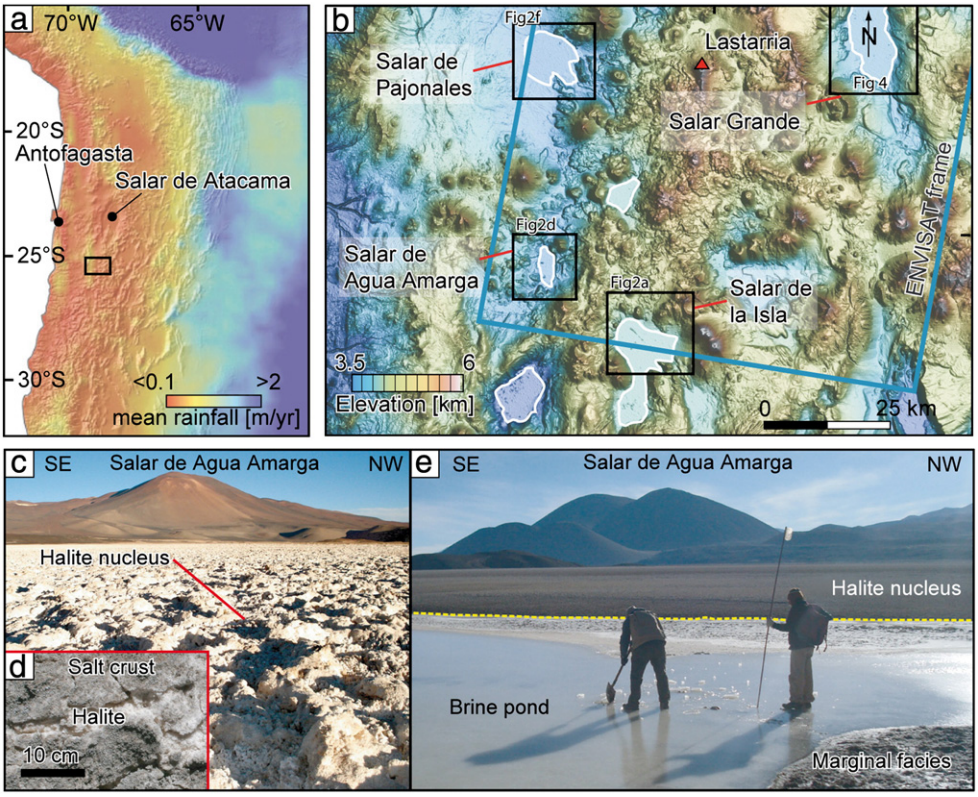

Fig. 1. The studied salars are located ~200 km south of Salar de Atacama and 250 km SE of Antofagasta city. a) Shaded relief map of the central Andes overlain by annual rainfall; the black rectangle indicates the position of the study area. b) DEM of the South Puna Plateau with salar locations, thick light grey boundary outlines the area covered by the InSAR time series, small black boxes delineate the studied areas of Figs. 2 and 4. Surface geology photographs at Salar de Amarga that show c) irregular hummocky surface of the halite nucleus facies, and d) flat surface of marginal facies (partially covered by frozen brine) with the transition to the more elevated surface of the halite nucleus.
Panel a: modified from Strecker et al. (2007).

surface and the associated halite bed is typically metres to ten or more metres thick. In plan view, a salar's hydrologically-controlled sediment system consists of two principal parts: a halite nucleus and a marginal salt flat zone (Fig. 1c–d), with respective proportions of the two varying from one salar to another (Houston, 2006; Lowenstein et al., 2003; Warren, 2006). Compared to the marginal zone, the surface of the halite nucleus is hummocky and rugose, it defines the region in the salar's central sump that is somewhat higher (tens of cm) than the immediately surrounding margin facies (Fig. 1c–e). This elevated halite nucleus facies is very rarely covered by a water sheet. This is unlike portions of the salar edges, where saline brines seep to the surface and can form brine-filled ponds and pits.

Directly below its surface (first few cm below), the halite nucleus facies is composed of an aggregated set of dry silty-cemented solution-etched salt encrustations. Below this, numerous mm–cm scale halite crystals are precipitating from capillary pore brines in a permeable halite mass. Solar-driven evaporation (not cryogenic concentration) drives an ongoing supply of brine to the nucleus, fed from the shallow water table and brought to the near surface by capillary forces. Salt etching in the uppermost layer of the halite nucleus is a response to occasional fogs and mists, which in this hyperarid desert can constitute the main mode of fresh water influx to the elevated salar nucleus facies (Diaz et al., 1999). However, in terms of salar's solute budget, most of the ions precipitated as salts in the nucleus unit are groundwater-derived; this is why lithium salts can be recovered economically from pore brines in the halite nucleus facies across a number of Andean salars (Warren, 2010).

Adjacent marginal facies are made up of varying combinations of silty mudflats, saline pan crusts and brine ponds, with elevated proportions of gypsum and carbonate minerals in the underlying sediment, but with a sediment surface that for much of a year is still covered by fluffy white halite-rich effloresences and thin salt crusts (Fig. 1d). Occasional storm floods and alluvial sheet flood processes carry in much of the terrigenous mud and silt sediment found in the marginal facies. When flooded, the salt effloresences capping the marginal flats dissolve back into the covering brine sheets. With desiccation, this recycled salt can reform as a thin salt crust covering the lower parts of the surface in the marginal facies belt.

Small perennial brine ponds (lagunas and *ojo de diablo*) are brine-filled zones of salt dissolution (salt sinkholes), which are typically interspersed within the marginal facies of many Andean salars. In less-saline salar systems, or in zones of fault-controlled stronger groundwater resurgence, these perennial brine ponds and pits can occur also in the more central parts of a salar (Lowenstein et al., 2003; Warren, 2006).

2. Salar surface deformation analysis

To analyse the surface deformation, we use an interferometric synthetic aperture radar (InSAR) dataset acquired by the ENVISAT satellite composed of 21 images in descending orbit spanning from March 2003 to January 2008. By processing the phase difference (interferogram) between SAR image pairs separated in time, we obtain temporal and spatial surface displacements projected in the LOS (satellite line-of-sight) direction (e.g. Massonet and Feigl, 1998). We computed a total of 153 interferograms characterised by spatial baseline values smaller than 500 m. We applied the SBAS algorithm (see for details Berardino et al., 2002) to obtain mean deformation velocity maps and time series. The average standard deviation of the technique is generally 0.1–0.2 cm/yr for the velocity and 0.5–1 cm for the time series (Casu et al., 2006). Note that radar signal acquisition of superficial water (i.e. brine ponds and perennial lakes) will result in incoherence. This

means that in case of seasonal flooding during the SAR acquisition, those areas are incoherent.

Within the SAR satellite scene (24–25S and 67–68W) covering an area of ~10^3 km^2, we count a total of 12 salars of different sizes (from few km^2 up to 150 km^2 for Salar de la Isla). The elevation of the studied area ranges from 3500 m (salar de Pajonales) up to 5700 m (Lastarria volcano; Fig. 1b) above sea level. We observe that all 12 salars are deforming, with rates greater in some areas of some salars; the ground

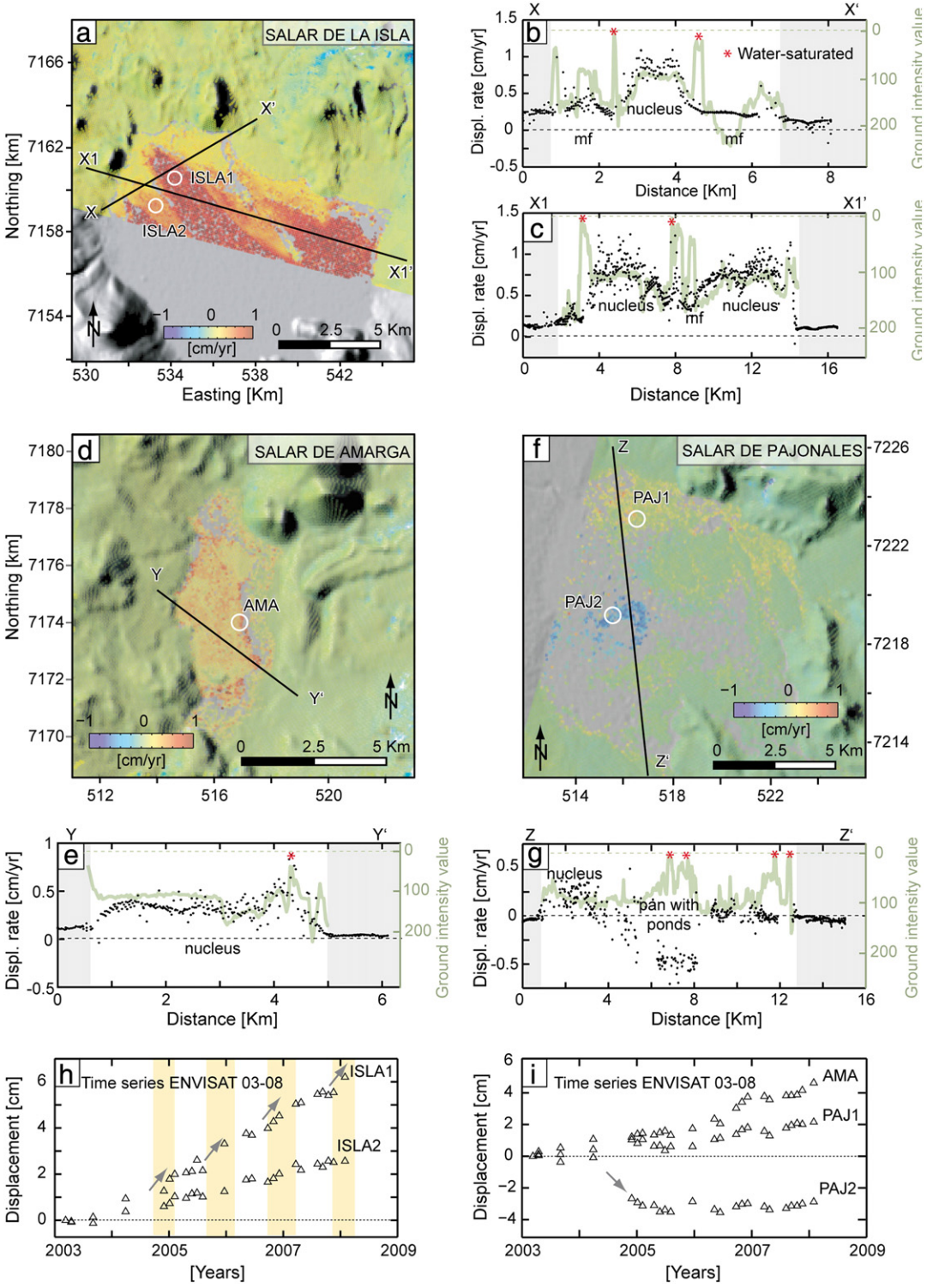

Fig. 2. InSAR observations (ENVISAT satellite, track 282, frame 4118) during the period from 2003 to 2008 at a) Salar de la Isla, with b) and c) that are the profiles across the InSAR velocity map (black dots) and across LANDSAT image intensity values (green line; near-IR, band 7, 10/11/2000) indicative of ground composition; red stars indicate localised superficial water bodies. Sampling width of the cross sections is 150 m. d) Salar de Agua Amarga and e) velocity profile across the InSAR dataset (black dots) and intensity values (green line) across LANDSAT images. f) Salar de Pajonales with g) velocity profiles across the InSAR dataset (black dots) and intensity values (green line) across LANDSAT images. All profile transects are shown as black lines on the deformation maps, while the thick light grey bars in e) and g) define the supra-shorezone positions on the salar profile; mf: marginal facies. Time series plot (sampled at white circle locations) at h) Salar de Isla, with vertical orange bars and grey arrows indicating possible seasonal acceleration phases, most clearly visible in ISLA1 profile, and i) time series at Salar de Pajonales and Salar de Amarga. (For interpretation of the references to color in this figure legend, the reader is referred to the web version of this article.)

displacement is negligible landward of the salar shorezone (green areas; Fig. 2a, d, f). Although the general location of the salars is found in volcanically and tectonically active areas, salar behaviour appears isolated from these systems in the given dataset. But, as we shall see, differences in elevation rates with various salars are associated with variation in hydrological style and inherent rates of groundwater transmissivity. By conducting more detailed analyses, three salars (Salar de la Isla, Salar de Agua Amarga and Salar de Pajonales) illustrate diverse relative proportions of surface facies, uplift or subsidence occurrences.

The northern portion of Salar de la Isla (25.7S 68.6W) has a maximum vertical displacement rate twice that of the other salars during the period of observation. Within the Salar de la Isla, two different rates are clearly observed at the salar surface (Fig. 2a) and along the velocity profiles (Fig. 2b–c) with velocities from 0.5 up to 1.5 cm/yr. These profiles show pronounced velocity gradient transitions from the shore into the salar, transiting from 0 on the periphery to around 1.3 cm/yr atop the halite nucleus, across a lateral distance of few hundred metres (Fig. 2c).

In Salar de Agua Amarga (25.54E, 68.84W), a transition from the shore to the salar is also evident (Fig. 2d). The velocity profile intersects part of a narrow circumferential perimeter to the nucleus showing higher deformation velocities at km 4 (Fig. 2e). This narrow perimeter corresponds to the sedimentary boundary between the halite nucleus and the marginal facies associations in the salar. Note that the halite nucleus surface is characterised by a series of subfacies, some being more hydrated (faster displacement velocities), or less hydrated (slower displacement velocities), in agreement with field data and Landsat images (Fig. 3). Overall, the halite nucleus surface is not rising as fast in this salar as in Salar de la Isla.

Portions of all three salars surveyed show some evidence of surface deformation or aggradation (Fig. 2a–g); however, the central part of Salar de Pajonales (25.14S, 68.80W) is different. There, the InSAR signal locally shows subsidence, and forms an annular-shaped geometry (Fig. 2f). The velocity profile shows from the N to the S, a transition from 0.5 cm/yr to −0.5 cm/yr (Fig. 2g). This salar has a reduced halite nucleus and has a surface characterised by dissolution lagoons and ponds, interspersed with gypsum pan crusts. This association of degradation features across the salar surface, and the presence of a dominant marginal facies association of sedimentary features over much of the salar surface (Fig. 3b), suggest that saline sediment is being lost at a relatively high rate, by passage of solutes into the regional groundwater system.

To analyse possible relationships between InSAR observation and local geology we compare profiles sampled across the InSAR dataset with profiles across optical images acquired by the LANDSAT satellite in 2006 (see Fig. 3 for profile locations). We use the band 7

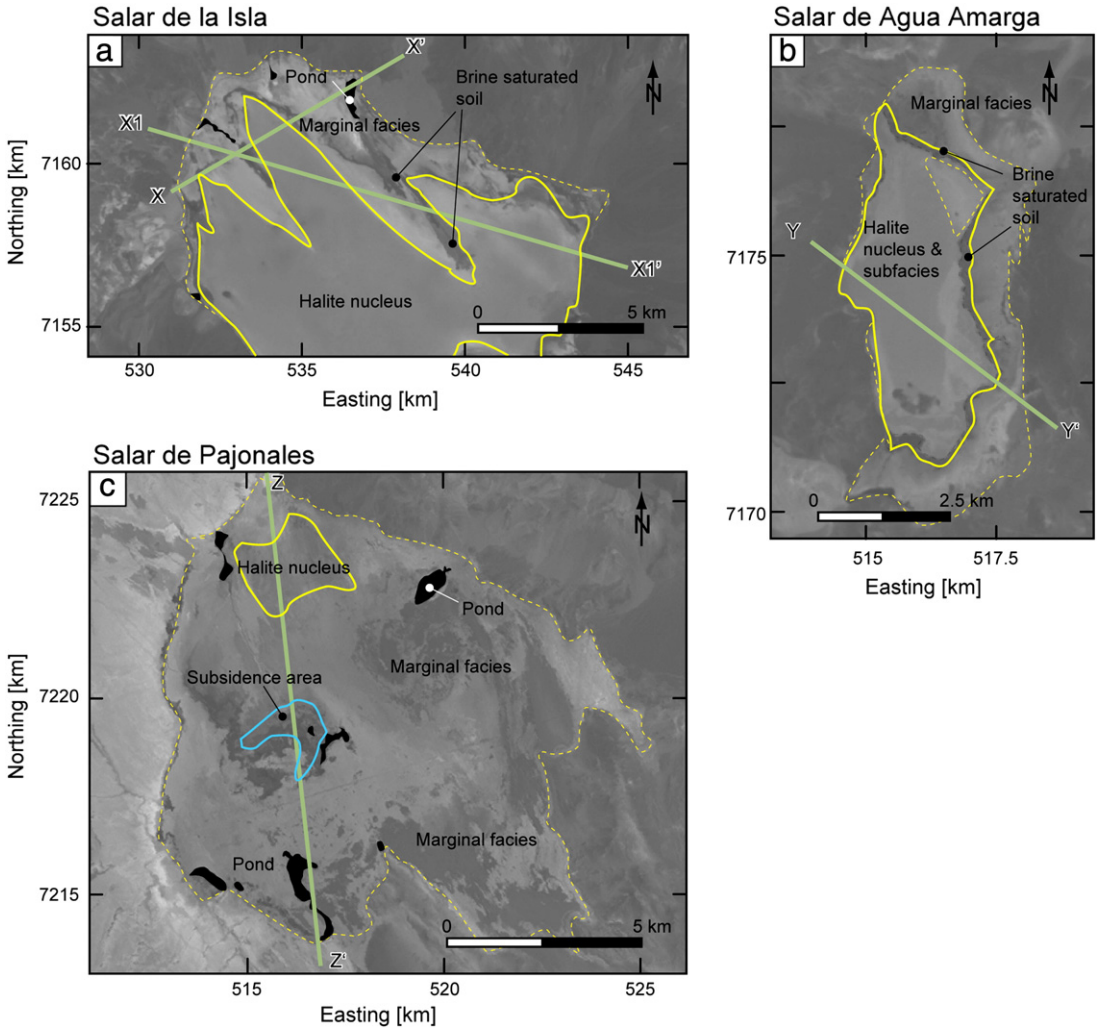

Fig. 3. Broad sedimentological facies distribution overlaid on LANDSAT band 7 (near-infrared; acquisition in 2006) at a) salar de la Isla; b) salar de Amarga, and c) salar de Pajonales. Thick yellow line is the halite nucleus periphery, dashed yellow line is the periphery of the marginal facies, and thick light blue line is the area where subsidence has been observed using InSAR (see main text for details). Black areas are ponds and laguna (superficial brine). Note that to observe a possible salar surface change in the last decades, we also analyse LANDSAT acquisitions from 1973 up to 2005. The surface geology shows an overall similarity, without noticeable surface modifications. (For interpretation of the references to color in this figure legend, the reader is referred to the web version of this article.)

(mid-infrared), and first find that the areas with weaker InSAR uplift signal (see ISLA2, Fig. 2a) correspond in LANDSAT to higher ground intensity values (close to white; All channels are quantized to a 0–255 scale, with zero equal to black and 255 to white). White areas in the LANDSAT images geologically match with the marginal facies, where much of the more marginward flat surface is covered by gypsum crusts. Second, the areas with larger uplift signals (see ISLA1, Fig. 2a) have lower ground intensity values in the LANDSAT images that correspond to the halite nucleus, where salt typically precipitates by capillarity from shallow groundwater bodies. Profiles across both InSAR velocity maps and LANDSAT mid-infrared intensity show that radar and optic signals are in good agreement (Fig. 2b, c, e), where the maximum uplift agrees with halite-rich nuclei prone to salt accretion. Localised peaks in the ground intensity values that tend to zero (red stars, Fig. 2b, c, e) correspond to perennial lakes, with the InSAR signal being incoherent due to the presence of water.

To analyse the temporal evolution of the salar surface, we compiled displacement time series on selected areas from 2003 to 2008 (Fig. 2h–i). ISLA1 (atop halite nucleus facies) and ISLA2 (atop marginal facies) are both located at the northern end of Salar de la Isla (white circles; Fig. 2a–c). They show different cumulative displacements sampled on two well-delimited facies zones, with mean values of 2 cm and 6.5 cm, respectively. This implies aggradation of both the marginal facies and the halite nucleus facies in this salar, with aggradation rates greater atop the halite nucleus facies association. Moreover, we observed cyclic displacement changes (mini uplifts) approximately from September to March each year, best expressed on the halite nucleus at Isla (ISLA1, Fig. 2h).

PAJ1 is located in the northern part of the Salar de Pajonales (white circle; Fig. 2f) and shows a comparable displacement trend with respect to ISLA2, with a cumulative displacement of 2 cm in almost 5 years. However, PAJ2, atop a zone characterised by sedimentary features indicative of local dissolution (marginal facies separated by numerous brine ponds), shows a clear signal subject to a rapid negative displacement along the LOS direction during the first trimester of 2004, for a duration of almost one year. Note that after 2006, the signal follows again a similar ground displacement comparable with areas of PAJ1 and AMA, the latter being located on the Salar de Amarga, 50 km distant, south east from Pajonales (Fig. 2d, f). This subsidence is probably not related to seasonal effects, because it is not observed in neighbouring salars.

Our observations are taken over a short period of time (about 5 years) in the salars' depositional histories. However, a second InSAR dataset using ERS satellite was processed (same as Ruch et al., 2009). By combining ERS with ENVISAT data, we observe a similar linear ground deformation over more than 10 years at the salar Grande from 1995 to 2008 (25.03S, 68.15W; see Fig. 1a for location; Fig. 4). This observation was not extended to the other three studied salars due to a spatial offset between the two satellite scenes, hence the intersected area contains only Salar Grande.

3. Discussion

In this study, we present a detailed analysis on salar ground displacement using geodetic and geological observations, together with chemical data in the Atacama Desert in Chile. We show that all salars observed are actively deforming and rates of deformation are directly related to broad sedimentological facies in the evaporite units in a salar. Our analysis demonstrates a strong intra- and inter-salar association between saline facies distribution and rates of rise or fall of the salar surface.

Despite the significance of salars as indicators of a set of hydrologic and evaporite processes, previous environmental and biologic studies have not used the evidence of sedimentological textures in the salar evaporites. Yet, because evaporite textures indicate hydrology (Warren, 2006), they can be used to interpret the likely hydrologic processes driving surface elevation changes.

In the broadest hydrological terms, the regional setting for the three salar hydrologies can be tied back to differences in groundwater transmissivity in the lithologies beneath and around the salars. The central halite-rich parts of Salar de Isla and Salar de la Agua Amarga are accreting. In contrast the surface across Salar de Pajonales shows evidence of dissolution, it is degrading and regionally it is underlain by a series of clastic alluvial sediments. The contrast between these three nearby salars, in what is a single ET (alpine tundra) Koeppen climate zone (Kottek et al., 2006), argues that the groundwater supply system may vary. It is probably somewhat leaky in the bajada clastics below the western margin of Pajonales (margin of the active volcanic arc), compared to the volcanic-enclosed hydrologically-closed base to the other two salars (Fig. 1b).

To confirm likely hydrological drivers to the varying rates of ground displacement within and between salars phenomena, the sedimentological and InSAR results are compared to chemical analysis of surface waters, from both water inflow and laguna locations, which were systematically sampled across the Andes in 1991 (Risacher and Fritz, 1991; Risacher et al., 2003). Although there are no pore water samples in the nucleus facies in the salars under study, brine samples from the salar edges confirm that the salar with the highest ground displacement rate of all salars observed, Salar de la Isla, also contains surface waters with the highest salinities in this section of the central Andes. Its maximum salinity is 330 g/l, significantly more than at Pajonales (247 g/l) than at Agua Amarga (197 g/l), hence, it is more prone to salt precipitation and associated ground deformation, and this likely explains its higher deformation rate.

Earlier studies of salars have suggested tectonically or fault-related ground motion can drive elevation changes in the salars (Reutter et al., 2006), while others propose an uplift and subsidence related to unloading, or the reduction of the water column (Bills et al., 1994), while yet others attribute in-salar elevation changes it to climate change and/or ice lens development in elevated saline lakes (Hurlbert and Chang, 1988). Historically, all these early studies have failed to match the hydrological style indicated by the evaporite distribution within the salar to the specific regions where different rates of elevation change are occurring. For example, if tectonic uplift was driving changes in elevation across a salar surface, elevation changes would not match the presence or absence and the undulating edges of the halite nucleus in all imaged parts of the salar. Rather, changes would relate to fault position and regional tilting and shifting of the active saline sump within the salar depression. At the millennial scale, tectonic tilting can change the regional salar hydrology, as seen in the changes in the salt sump position being driven by tilting in Salar de Atacama (Bobst et al., 2001; Jordan et al., 2002) but it does not explain the cm/year scale of accretion observed in the imaged salars.

It was proposed that ice heave may control salar elevation changes (Hurlbert and Chang, 1988). If so, ice sheets would have to be a dominant feature within the halite nucleus area, where the InSAR analysis shows most of the elevation changes occur. However, the halite nuclei in all Andean salars lack evidence of pervasive intrasediment ice sheets. If an ice sheet ever did form in the halite nucleus area, it could only form atop or very near to the nucleus surface (freezing water is less dense than a halite saturated pore brine). No such feature has ever been documented in any Andean halite nucleus. If any cryogenically precipitated mineral salts ever formed substantial salt masses within a halite nucleus, they would leave behind widespread characteristic mineral fingerprints; such as, cold season hydrohalite, mirabilite, thernardite, glauberite, and epsomite (Warren, 2010). None of these cryogenic indictor salts is commonplace in the halite nucleus of any Andean salar.

Another possible alternative to capillary evaporation driving aggradation is a variable distribution of hygroscopic material (i.e. clays or hydroscopic salts) in the salar depression, which may induce local ground swelling and thus ground displacement in response to periodic

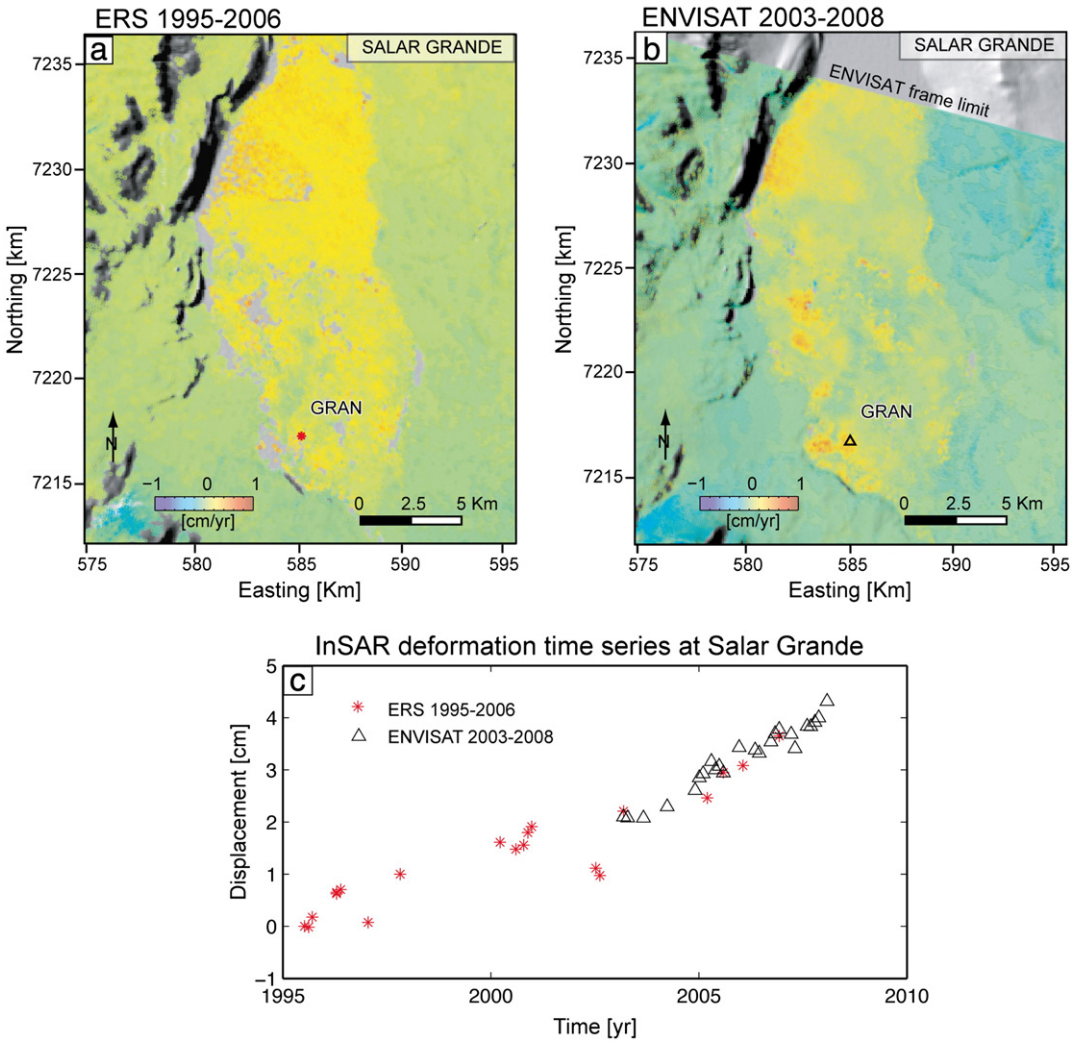

Fig. 4. Deformation map at Salar Grande, central Andes (for location, see Fig. 1b; up right corner). a) Shaded relief maps with InSAR observations for b) the period from June 1995 to December 2006 (ERS satellite) and c) the period from April 2003 to January 2008 (ENVISAT satellite). c) Time series plot for the ERS (red stars) and ENVISAT (black triangles) datasets for an observation point at the salar centre. Results show an almost linear increase of the signal with a good agreement between the two datasets. (For interpretation of the references to color in this figure legend, the reader is referred to the web version of this article.)

water influx to the salar system (Gabriel et al., 1989). However the better tie of the InSAR rates to the at-surface expressions of evaporite hydrology (halite nucleus versus margin flat versus salt karst) suggests the relative rates of rise of the various salar evaporite surfaces are more responses to a hydrologically, not hydroscopically, driven set of arid-zone processes. The predominant salt texture present in the halite nucleus is medium to coarsely crystalline halite aggregates and clusters. When halite acts best as a hydroscopic salt it tends to be fine grained with the resulting increased surface area greatly aiding its hydroscopic capacity. Other highly deliquescent salts (such as the calcium chloride salts or the potash salts) are not present in sufficient volumes to explain the elevated rates of aggradation in the nucleus. If hydroscopic clay is the main driver, then the highest rates of aggradation would not be confined to the halite nucleus.

Given these observations, we are led to the following conclusions:

(a) Mechanisms of salar deformation: our results suggest that the ground deformation observed in the salars is likely related to regions of salt accumulation immediately beneath a surface of salt encrustation, especially within the halite nucleus where capillary halite precipitation dominates (Fig. 5). The rate observed with InSAR is in agreement with rock-core based estimates of short-term halite precipitation rates of 0.3–3.6 m/kyr in the halite nucleus facies in Salar de Atacama (Lowenstein et al., 2003). Thus, ongoing salt precipitation in the halite nucleus induces a volume increase that is evidenced by surface deformation. InSAR, thus measures the superficial salt crust deformation, likely induced by shallow halite precipitation in the zone beneath (Fig. 5). The salar surface is then raised, in response to the increasing salt volume precipitating below; much in the same way the surface the Abu Dhabi coastal salt flat (sabkha) is raised by the precipitation of $CaSO_4$ in the coastal capillary zone (Wood et al., 2002).

In this study, we focused on a saline area measuring ~ 100×100 km, but we suggest that the observations we make may be applied to other similar saline facies across the central Andes. This type of approach, matching InSAR elevation data to evaporite sediment facies in order to remotely confirm near surface capillary concentration of brines contrasted with regions of net salt loss, most likely has application in continental saline sumps worldwide (Australia, North Africa, the Middle East, Tibet and North America).

(b) Time dependence of salar deformation: we document mean values of salar surface uplift of up to 1.5 cm/yr. This is one order of magnitude more compared to the upper boundary estimations for the long-term deformation (10 ky), registered in Salar de

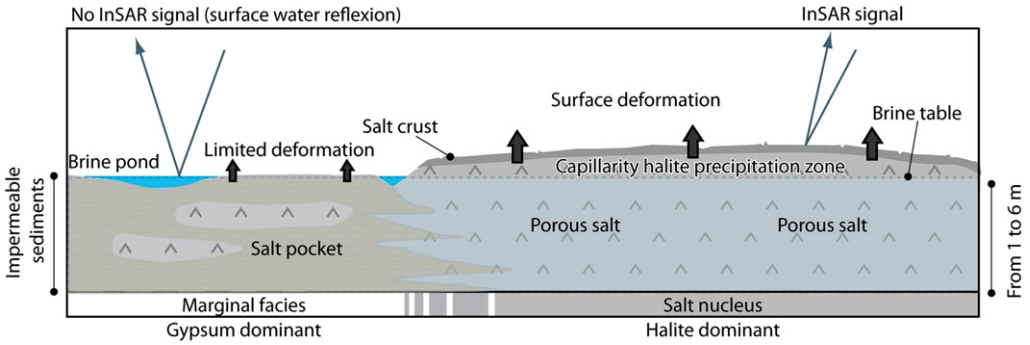

Fig. 5. Interpretative profile across a salar.
Modified from Risacher and Fritz (2009).

Atacama (up to 0.18 cm/yr; Bobst et al., 2001). Lowenstein et al. (2003), however, observed strong spatial variations of the deformation rate (up to 0.38 cm/yr for the Pleistocene). The latter value corresponding to the mean velocity observed at the marginal facies in our observations. This difference may be explained by surface dissolution occurring during wetter periods that may strongly bias the long-term deformation estimations. The system is located in a hyperarid desert, which by definition will experience significant mega-flood events many years apart (and not one occurred in the time frame of our InSAR measurements). If a constant ground displacement (aggradation) rate of >1 cm/yr (as observed at Salar de la Isla) had continued over a century or more, we would expect the precipitation of halite in the nucleus facies to induce a height differential of around 1 m/century compared to the aggradation rate of the marginal facies. This is not the case, field observation at Isla and at other salars across the Altiplano indicate that only few tens of centimetres separate the surfaces of the halite nucleus and the margin facies associations, indicating likely variation in the salar surface inflow dynamics in the recent past. Transient strong rain or snowfall events on time scales greater than our few years of observation (Ortlieb, 1995), and perhaps periodic dripping fogs, must influence the heights of differentials across the various salar surfaces. In addition, the regional diminution of the permafrost elevation, as observed over decades in the Andes (Romanovsky et al., 2007; Trombotto, 2000) may contribute to an increase in the annual volume of incoming groundwater. In the long-term, a rising brine table, that was previously at a lower level, will increase the accommodation space for the evaporite nucleus and so raise the salar surface, allowing beds to capillary salt to accumulate in the salar depression.

4. Conclusions

We use InSAR time series for the period from 2003 to 2006, optic images and field observations to analyse salar deformation in the Atacama Desert in Chile (24–26°S). We find that all salars present in the surveyed area are deforming at rates of up to 1.5 cm/yr, with the higher rates corresponding to the distribution of the halite nucleus facies. Our analysis shows that broad sediment facies can be related to InSAR-determined surface deformation (velocity profiles and time series analysis), implying an underlying hydrologic/sedimentologic control. To explain the salar deformation, we propose a conceptual model related to capillary halite precipitation that develops in and immediately below a superficial salt crust. Our observations have significant implications in terms of: a) development of remote techniques for recognition of movable near-surface water on Earth and potentially in extraterrestrial settings; b) recognition of hydrologic stability/climatic variability preserved in the infill beds as variable salt signatures; c) identification of regions of likely concentration of particular solute components in salar pore brines, such as lithium and boron. The fact that salar surfaces are aggrading at different rates, both within and between salars, has direct geohydrologic and indirect long-term climatic implications.

Acknowledgments

The authors acknowledge Matt Pritchard and Jack Loveless for their constructive reviews, Tom Carpenter for providing field photographs. ENVISAT data were provided by the ESA as part of CAT-1 project # 3455. The research was partially funded by the DFG, grant # WA1642.

References

Alonso, R.N., Jordan, T.E., Tabbutt, K.T., Vandervoort, D.S., 1991. Giant evaporite belts of the Neogene central Andes. Geology 19 (4), 401–404.
Berardino, P., Fornaro, G., Lanari, R., Sansosti, E., 2002. A new algorithm for surface deformation monitoring based on small baseline differential SAR interferograms. IEEE Trans. Geosci. Remote. Sens. 40 (11), 2375–2383.
Betancourt, J.L., Latorre, C., Rech, J.A., Quade, J., Rylander, K.A., 2000. A 22,000-year record of monsoonal precipitation from Northern Chile's Atacama desert. Science 289 (5484), 1542–1546.
Bills, B.G., de Silva, S.L., Currey, D.R., Emenger, R.S., Lillquist, K.D., Donnellan, A., Worden, B., 1994. Hydro-isostatic deflection and tectonic tilting in the central Andes: initial results of a GPS survey of Lake Minchin shorelines. Geophys. Res. Lett. 21, 4. doi:10.1029/93GL03544.
Bobst, A.L., Lowenstein, T.K., Jordan, T.E., Godfrey, L.V., Hein, M.C., Ku, T.L., Luo, S., 2001. A 106 ka paleoclimate record from the Salar de Atacama, northern Chile. Palaeogeogr. Palaeoclimatol. Palaeoecol. 173, 21–42.
Casu, F., Manzo, M., Lanari, R., 2006. A quantitative assessment of the SBAS algorithm performance for surface deformation retrieval from DInSAR data. Remote Sens. Environ. 102 (3–4), 195–210.
Diaz, G.C., Mendoza, M., Garcia-Veigas, J., Pueyo, J.J., Turner, P., 1999. Evolution and geochemical signatures in a Neogene forearc evaporitic basin: the Salar Grande (Central Andes of Chile). Palaeogeogr. Palaeoclimatol. Palaeoecol. 151, 39–54.
Gabriel, A.K., Goldstein, R.M., Zebcker, H.A., 1989. Mapping small elevation changes over large areas: differential radar interferometry. J. Geophys. Res. 94, 9183–9191.
Houston, J., 2006. Evaporation in the Atacama Desert: an empirical study of spatio-temporal variations and their causes. J. Hydrol. 330 (3–4), 402–412.
Hurlbert, S.H., Chang, C.C.Y., 1988. Distribution, structure, composition and thermal environment of ice deposits in Andean salt lakes. Hydrobiologia 158, 271–299.
Jordan, T.E., Muñoz, N., Hein, M., Lowenstein, T.K., Godfrey, L., Yu, J., 2002. Active faulting and folding without topographic expression in an evaporite basin, Chile. Geol. Soc. Am. Bull. 114, 1406–1421.
Kottek, M., Grieser, J., Beck, C., Rudolf, B., Rubel, F., 2006. World map of the Köppen–Geiger climate classification updated. Meteorol. Z. 15, 259–263.
Lowenstein, T.K., Hardie, L.A., 1985. Criteria for the recognition of salt-pan evaporates. Sedimentology 32, 627–644.
Lowenstein, T.K., Hein, M.C., Bobst, A.L., Jordan, T.E., Ku, T.-L., Luo, S., 2003. An assessment of stratigraphic completeness in climate-sensitive closed-basin lake sediments: Salar de Atacama, Chile. J. Sediment. Res. 73, 91–104.
Massonet, D., Feigl, K.L., 1998. Radar interferometry and its applications to changes in the Earth's surface. Rev. Geophys. 36, 441–500.
Núñez, L., Grosjean, M., Cartajena, I., 2002. Human occupations and climate change in the Puna de Atacama, Chile. Science 298 (5594), 821–824.
Ortlieb, L., 1995. El Nino event and rainfall episodes in the Atacama Desert: the record of the last two centuries. Bull. Inst. Fr. Etud. Andin. 24 (3), 519–537.
Placzek, C., Quade, J., Patchett, P.J., 2006. Geochronology and stratigraphy of Late Pleistocene lake cycles on the Southern Bolivian Altiplano: implications for causes of tropical climate change. Geol. Soc. Am. Bull. 118, 515–532.
Pritchard, M.E., 2003. Recent crustal deformation in west central South America, Ph.D. thesis, Calif. Inst. Technol., Pasadena.

Quade, J., Rech, J.A., Betancourt, J.L., Latorre, C., Quade, B., Rylander, K.A., Fisher, T., 2008. Paleowetlands and regional climate change in the central Atacama Desert, northern Chile. Quat. Res. 69 (3), 343–360. doi:10.1016/j.yqres.2008.01.003.

Reutter, K.-J., Charrier, R., Götze, H.-J., Schurr, B., Wigger, P., Scheuber, E., Giese, P., Reuther, C.-D., Schmidt, S., Rietbrock, A., Chong, G., Belmonte-Pool, A., 2006. The Salar de Atacama Basin: a subsiding block within the western edge of the Altiplano–Puna Plateau. In: Oncken, O., Chong, G., Franz, G., Giese, P., Götze, H.-J., Ramos, V.A., Strecker, M.R., Wigger, P. (Eds.), The Andes — Active Subduction Orogeny. Frontiers in Earth Science Series, Vol. 1. Springer-Verlag, Berlin Heidelberg New York, pp. 303–326.

Risacher, F., Fritz, B., 1991. Geochemistry of Bolivian salars, Lipez, southern Altiplano: origin of solutes and brine evolution. Geochim. Cosmochim. Acta 55 (3), 687–705.

Risacher, F., Fritz, B., 2009. Origin of salts and brine evolution of Bolivian and Chilean salars. Aquat. Geochem. 15 (1), 123–157.

Risacher, F., Alonso, H., Salazar, C., 2003. The origin of brines and salts in Chilean salars: a hydrochemical review. Earth Sci. Rev. 63 (3–4), 249–293.

Romanovsky, V.E., Gruber, S., Instanes, A., Jin, H., Marchenko, S.S., Smith, S.L., Trombotto, D., Walter, K.M., 2007. Global Outlook for Ice and Snow: Frozen Ground Ch. 7 (Birkenland Trykkeri A/S, Norway).

Ruch, J., Manconi, A., Zeni, G., Solaro, G., Pepe, A., Walter, T.R., Lanari, R., 2009. Different deformation scales and stress field change in the Lazufre volcanic area, Central Andes. Geophys. Res. Lett. 36. doi:10.1029/2009GL041276.

Strecker, M.R., Alonso, R., Bookhagen, B., Carrapa, B., Hilley, G.E., Sobel, E.R., Trauth, M.H., 2007. Tectonics and climate of the Southern Central Andes. Ann. Rev. Earth Planet. Sci. 35, 747–787. doi:10.1146/annurev.earth.35.031306.140158.

Trombotto, D., 2000. Survey of cryogenic processes, periglacial forms and permafrost conditions in South America. Rev. Inst. Geol. 21 (1/2), 33–55.

Warren, J.K., 2006. Evaporites: Sediments, Resources and Hydrocarbons. Springer, Berlin. 1036 pp.

Warren, J.K., 2010. Evaporites through time: tectonic, climatic and eustatic controls in marine and nonmarine deposits. Earth Sci. Rev. 98, 217–268.

Wood, W.W., Sanford, W.E., Al Habshi, A.R.S., 2002. Source of solutes to the coastal sabkha of Abu Dhabi. Geol. Soc. Am. Bull. 114, 259–268.